

TRANSIENT THERMAL ANALYSIS OF SMALL SQUIRREL CAGE MOTOR THROUGH COUPLED FEA

ROMAN PECHANEK¹, VLADIMIR KINDL¹, BOHUMIL SKALA²

¹Faculty of Electrical Engineering
Regional Innovation Centre for Electrical Engineering
University of West Bohemia, Pilsen, Czech Republic

²Faculty of Electrical Engineering
University of West Bohemia, Pilsen, Czech Republic

e-mail: rpechane@rice.zcu.cz

The thermal analysis is necessary in design process of new electric motor. During motor design process is necessary to know temperatures of induction motor's (IM's) construction parts. The calculated temperatures in all motor parts should be lower than critical temperatures. This paper deals with free-dimensional (3D) transient thermal analysis of small squirrel cage motor/induction motor. The design of new IM is based on dimensions of permanent magnet synchronous motor (PMSM). In the initial stage of motor's design the coupled finite element analysis (FEA) method gives enough valuable results of the IM's temperature rise. Coupled thermal analysis is made through computational fluid dynamics (CFD) and finite element method (FEM). The CFD model of IM is used for calculate boundary condition such as heat transfer coefficient. Results of CFD model are implemented in to transient thermal analysis as boundary condition.

KEYWORDS

induction motors, machine modelling, thermal analysis, simulation, computational fluid dynamics, finite element analysis,

1. INTRODUCTION

All electrical machines generate losses in form of heat generation. Obviously, this quantity of heat must be cleared away to prevent damage of the machine. Furthermore, machine rating mainly depend on the thermal capability of the system. A lots of industry application problems of IMs relate to the thermal limitations of machine.

Nowadays, the squirrel cage induction motor is most common used as industrial drives. Main benefits of IM is simple design and construction. Further IM is characterized reliable operation, low initial cost, easy operation and maintenance, relatively high efficiency, etc. Because IM has very important position in industry therefore thermal analysis is required at designing process of new IM.

The maximizing use of electrical machines leads to an increase in electrical load of active components. Losses that arise in these parts, have resulted in increasing the temperature of active components, or the whole machine. This issue is important to address simultaneously the electromagnetic and mechanical design of IM. A magnetic circuit has similar, sort of limitations needed to be also took into account in machine design. From the above it is clear that identifying of the temperature of all critical parts is of key importance.

Because this type of electric machines has very important position in industry and has very significant advantages, numerous studies were presented in the field of thermal analysis of IM. [Alberti 2008], [Zhang 2012], [Trigeol 2006].

2. CALCULATION METHODS

2.1 Losses of Induction Motor

At thermal analysis of IM is necessary to know the values of the losses and their exact location in the motor. The calculation of losses is based on known dimensions and electrical parameters of IM. These

parameters are known from design stage. According this fact IM's losses are set by analytical method. All formulas for calculating losses are presented. IM's losses can be divided to I²R losses, iron core losses, additional losses and mechanical losses. The losses in magnetic circuit can be further divided into: eddy current and hysteresis losses, surface losses and the losses due to flux pulsation. [Kindl 2010] In simulation mechanical losses are neglected. Based on empirical relationships can be established only total mechanical losses. However there is a problem with their specific location and dividing in machine. They are therefore neglected. I²R losses in the stator and rotor windings are described by:

$$\Delta P = m \cdot (R_1 + R_2) \cdot I^2 \quad (1)$$

where m is number of phases, $R_{1,2}$ is stator/rotor winding resistance, I is supply current. Iron core losses are determined based on the relationship

$$\Delta P_{FEhj} = \Delta p_{1,0} \cdot \left(\frac{f}{50}\right)^\beta \cdot (k_{dq} \cdot B^2 \cdot m_j) \quad (2)$$

where $\Delta p_{1,0}$ is specific losses of used iron, f is supply frequency, β coefficient dependent on used lamination, k_{dq} is coefficient representing inhomogeneous flux density distribution, B is average flux density in division of magnetic circuit, m_j is weight of division of magnetic circuit.

Additional losses are considered as no-load losses incurred in:

Surface of iron core in air gap

$$\Delta P_{po} = \frac{\pi}{2} D_1 \cdot \alpha \cdot l_e \cdot k_0 \cdot \left(\frac{Q_{1,2} \cdot n}{10000}\right)^{1.5} (t_{d1,2} \cdot \beta_{0x} \cdot B_\delta \cdot k_c \cdot 1000)^2 \quad (3)$$

where D_1 is stator inner diameter, α is pole coverage coefficient, l_e is length of stator/rotor packet, k_0 is factor of surface loss, $Q_{1,2}$ is number of slots, n is RPM, $t_{d1,2}$ is slot pitch, β_δ is pulsation in the air gap flux density. For the stator teeth the β_{0x} depends on the ratio of slots opening and the air gap length. Similarly are set teeth losses due to pulsating magnetic flux

$$\Delta P_{p1,2} \approx 0.11 \cdot \left(\frac{Q_{1,2} \cdot n}{1000} \cdot B_{p1,2}\right)^2 \cdot m_{j1,2} \quad (4)$$

where $Q_{1,2}$ is number of slots, n is RPM, $m_{j1,2}$ is weight of stator/rotor teeth, $B_{p1,2}$ is magnitude of flux density saturating stator/rotor teeth.

2.2 Fluid Dynamics Model

The fluid flow calculation is the first indicator of the cooling capability of the electrical machine. The modeling of fluid flow generally are presented two basic approaches. Modelling through a lumped parameter method and through CFD methods. In presented paper is CFD method used. Simulation of coupled analysis is performed in software ANSYS. Due to this method is possible to simulate fluid flow by numerical solution of the Navier-Stokes equations. In principle, the Navier-Stokes equations describe both laminar and turbulent flows without the need for additional information. The turbulent flow is more often during a cooling process of electrical machine. [Koldzovski 2010], [Kuosu 2004], [Marignetti 2008]. Navier-Stokes equation and continuity equation for an incompressible fluid (5)

$$\rho \frac{\partial U}{\partial t} + \rho(U \cdot \nabla)U = -\nabla p + 2\nabla \cdot (\eta \nabla U) + f \quad (5)$$

$$\nabla U = 0$$

where ρ is density, U is speed, ∇ is Laplace operator, p is pressure, η is dynamic viscosity and f is volume force acting on the fluid.

Solving this equation is problematic because of the nonlinear inertia term which generates turbulence. Turbulence consists of fluctuations in the flow field in time and space. It is a complex process, mainly because it is three dimensional, unsteady and consists of many scales. It can have a significant effect on the characteristics of the flow. Turbulence occurs when the inertia forces in the fluid become significant compared

to viscous forces, and is characterized by a high Reynolds Number. In simulation is used $k - \epsilon$ model of turbulence. The $k - \epsilon$ model of turbulence introduces new variables into the system of equations. The momentum equation and continuity equation is then:

$$\rho \frac{\partial U}{\partial t} + \rho(U \cdot \nabla)U = -\nabla p' + \nabla \cdot (\mu_{eff}(\nabla U + (\nabla U)^T)) + f_{sum} \quad (6)$$

$$\nabla U = 0$$

where, p' is modified pressure, μ_{eff} is effective viscosity accounting for turbulence and f_{sum} is sum of body forces.

CFD analysis determines; velocity distribution of the flowing fluid, pressure distribution of the flowing fluid and natural and forced convection at cooling surfaces. The convective heat transfer is given by:

$$q = \pi \cdot d \cdot \lambda \cdot Nu(T_s - T_f). \quad (7)$$

Where q is heat flux, d is specific diameter of solid at boundary, λ is thermal conductivity of the fluid, T_s and T_f are temperatures of the solid body and fluid, and Nu is the Nusselt number given by:

$$Nu = 2 + 0.6 Re^{0.5} \left(\frac{\mu \cdot c}{\lambda} \right)^{\frac{1}{3}} \quad (8)$$

where μ is viscosity, c is specific heat of fluid.

2.3 Thermal Model

In general heat transfer takes place in three ways. First is heat conducting, second is heat convection and third is radiation. [Staton 2005], [Vlach 2010], [Hurska 2012] Presented thermal models of IM consider only solid conduction and air convection. Heat transfer by radiation is neglected, due to small values. If we assume transient thermal analysis Biot-Fourier equation is used. Biot-Fourier equation usually is called as power balance equation and can be written in form (9). The first term represents heat absorbed in heat capacity, second term represents heat flux conducted in to volume and last term is heat generation inside the volume.

$$\rho \cdot c \cdot \frac{\partial T}{\partial t} - \nabla \cdot (\lambda \cdot \nabla T) = Q \quad (9)$$

where ρ is density, c is specific heat capacity, T is temperature, t is time, Q is inner heat generation. Two types of boundary condition are usually presented in the thermal analysis. The first one is Dirichlet's condition. Dirichlet's boundary condition sets at solid body surface the constant temperature. The second type of boundary condition is Neuman's condition. This boundary conditions is represented by the heat transfer coefficient at the cooling surfaces. Heat transfer coefficient can be obtained by analytical method directly from Newton's law equation.

$$q = -\lambda \cdot \nabla T = h \cdot (T_s - T_f) \quad (10)$$

where h is heat transfer coefficient. In presented thermal analysis, calculation of heat transfer coefficient is made through CFD (7) and applied on surface between cooling air and cooled motor parts.

3. APPLICATIONS

3.1 IM's model

The application of the calculation methods described above is performed on a small IM. Design of IM is based on the requirement to replace the existing rotor of PMSM to squirrel cage rotor. Requirement of design is given by mains dimensions of PMSM. Outer diameter of the stator core respectively stator frame are defined by dimensions of PMSM. Number of stator slots has to be the same as number of stator slots in PMSM. Length of stator / rotor core could be modified during design process. Also nominal power of IM is identical to the nominal power of PMSM. Due to general lower efficiency of IM, is assumed increasing of operating temperatures. Designed IM model is presented at Fig. 1. IM is modeled by convection at outer frame surface. Mains of operating parameters are presented in Tab. 1. Clearly can be seen

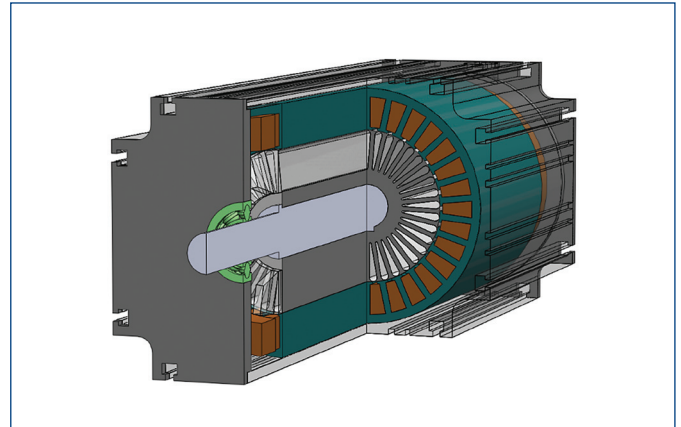


Figure 1. 3D model of new designed IM

rated power, rated current, rated voltage, rated speed and efficiency of IM. The value of efficiency consider all types of losses in IM from design stage.

At the Fig. 1. can be seen the main components of the IM in partial cross and axial section. The inner cooling air and the outlet boundary air do not show. Stator winding in straight part is modeled as one solid body, but random wound winding is designed originally. That been mention in chapter "3. 2 Geometry and material properties of IM". Rotor winding is presented aluminum bars.

Item	Value	
Rated power	9	kW
Rated stator current	220	A
Rated voltage	33	V
Rated speed	3000	RPM
Efficiency	93.7	%

Table 1. Specification of IM

Thermal analysis of the IM is carried out according to simulation diagram Fig. 2. The weakly coupled algorithm considers no back affecting (one-way coupling) of participated fields. This method contains two computation steps. In the first step the fluid flow field is calculated and transferred as boundary condition in the thermal analysis. It is essentially a special (feedback less) case of partially coupled field analysis.

3.2 Geometry and material properties of IM

The main dimension parameters of 9kW IM as frame length, frame diameter, number of slots and atc. are presented in Tab. 2. The outer diameter of stator core respectively stator frame are defined by dimensions of PMSM. Length of stator/rotor core could be modified during design of IM. As well known, to reduction computation time the electrical machine models are usually portioned out into smaller symmetrical parts. This fact leads to decrease the number of mesh elements and indeed to reduction of computation time. But unfortunately, this simplification cannot be done in the study of coupled thermal analysis. In this case CFD need to be directly coupled with FEM. This is reason, why simplified model cannot be calculated. Inner

Item	Value		
Frame length	L	0.4	m
Frame diameter	D_e	0.15	m
Rotor outlet diameter	D_i	0.08	m
Number of stator slots	Q_1	30	-
Number of rotor slots	Q_2	37	-

Table 2. Main geometry of IM

cooling air is modeled separately as auxiliary part of motor solid body. Outer air is modeled as ambient enclosure.

Thermal parameters of machine parts are presented in Tab. 3. The computational model is in 3D. This fact allows to set different material properties in different directions. One of the most important parameter is thermal conductivity of stator winding. At original stator winding comprises of insulated wire. Insulated wire is placed in insulated slots. In 3D mathematical model is winding simplified into one volume. That means equivalent thermal conductivity of stator winding have to be defined. The equivalent thermal conductivity of windings is set by relation

$$\lambda_w = \frac{\delta_1 + \delta_2 + \dots + \delta_n}{\frac{\delta_1}{\lambda_1} + \frac{\delta_2}{\lambda_2} + \dots + \frac{\delta_n}{\lambda_n}} = \frac{\sum_{i=1}^n \delta_i}{\sum_{i=1}^n \frac{\delta_i}{\lambda_i}} = \frac{\sum_{i=1}^n \delta_i}{\sum_{i=1}^n \frac{1}{\alpha_{wi}}} \quad (11)$$

where λ_w is equivalent thermal conductivity of winding, δ is length of windings parts.

Material	Thermal conductivity [W/mK]	Specific heat [J/kgK]	Density [kg/m ³]
Stator winding	$k_x = 2$ $k_y = 4$ $k_z = 380$	390	8900
Stator core	$k_x = 40$ $k_y = 40$ $k_z = 2$	460	7900
Rotor squirrel cage	160	870	2270
Rotor core	$k_x = 40$ $k_y = 40$ $k_z = 2$	460	7900-
Frame	160	870	2270
Air	0.03	1000	1.3

Table 3. Material data of IM

3.3 Loads and Boundary Conditions

In the case of thermal analysis, loads are presented by I²R losses in motor windings and losses in magnetic circuit. All thermal loads are calculated according analytical methods described in chapter 2.1. Thermal load are presented in Tab. 4.

Item	Value	
Rotor speed	3 000	RPM
I ² R stator losses	143.20	W
Iron core losses	100.63	W
I ² R rotor losses	125.97	W
Addy losses	135.35	W

Table 4. Thermal loads of IM

Mechanical losses are neglected since their determination is uncertain in the calculation. Furthermore, it is not sufficient accuracy found a parts of the machine, where mechanical losses arises. Neglect of mechanical losses in simulation is seen as a zero heat source in the bearings. This concept is not correct with the physical theory. But in the case that more important is the calculation of the stator winding temperature, can be mechanical losses neglected. The value of mechanical losses in the design stage was set to 98W.

Boundary condition of thermal analysis are calculated through CDF and implement at cooling surface of machine. This fact leads to reduce calculating time. Initial temperature of transient thermal analysis is $T_{amb} = 0^\circ\text{C}$.

In the case of CFD simulation. Two calculations are presented first is inner air, second is outer cooling air. The model of inner air of the motor represents convection heat transfer from rotor parts to IM frame, and heat

transfer through air gap of IM. Model of outer cooling air describes heat convection to ambient air. Boundary conditions of inner air CFD model are walls with equivalent friction $f = 0.01$ mm and with heat transfer. Inner calculation model in addition include rotating parts. Prerequisite are set rotating wall as boundary condition. Outer cooling air volume, the boundary conditions are set as wall with equivalent friction $f = 0.01$ mm and with heat transfer at border of machine frame and cooling air. Also "Opening" boundary condition is used at outer faces of air volume. "Relative Pressure" is set to 1 Pa and "Opening Temperature" is set to 0°C . Presented process corresponds with solving diagram at Fig. 2.

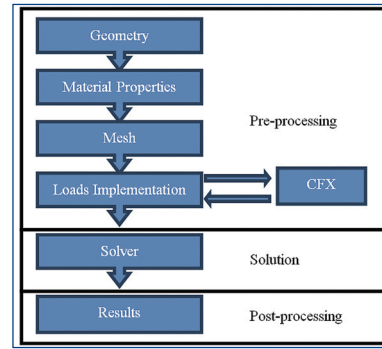


Figure 2. Simulation diagram

4. RESULTS

At this place transient thermal analysis results of small IM are presented. Results are presented for nominal load 9 kW and nominal speed of machine 3000 RPM. We assume that all thermal heating move from motor by frame surface. Due to this fact two types of simulation results are presented at this chapter. First results from CFD analysis. That results are presented by heat transfer coefficient on frame of IM see Fig. 3. This result are directly coupled to transient thermal analysis.

Heat transfer coefficient at outer surface of IM frame are in range $h = 13 - 17 \text{ Wm}^2/\text{K}$. Heat transfer coefficient at inner surface depends on rotating speed respectively at air flow speed. At rotating surface heat transfer coefficient are in range $h = 60 - 120 \text{ Wm}^2/\text{K}$. The heat transfer coefficient at stationary surface reach lower values $h = 45 - 70 \text{ Wm}^2/\text{K}$.

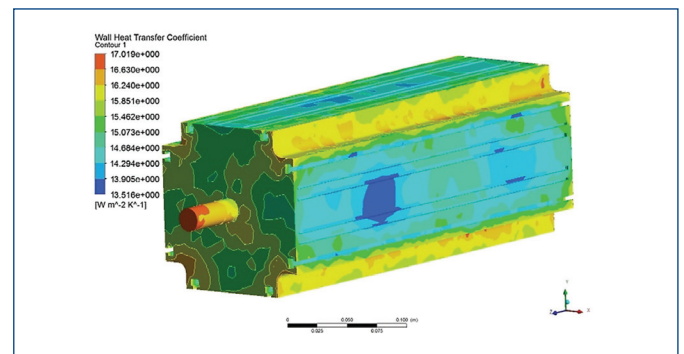


Figure 3. Heat transfer coefficient

Second presented types of results are transient thermal analysis results. Simulation was starting from cold (ambient) temperature $T_{amb} = 0^\circ\text{C}$. The simulation of temperature rise takes 1 hour. After this time the operating temperature of IM stabilizes. The time step are set to 60 seconds. IM at cross and axial section is presented at Fig. 4.

Fig. 4. shows IM place with the lowest and highest final temperatures. Locations with the lowest steady-state temperature is bearing, bearing shields and motor frame. The steady-state temperature of bearing shields are 124°C . The highest final temperature of stator frame is 132°C .

The final temperature distributions at the stator geometry is presented in Fig. 5. Figure shows the difference in temperature of the stator

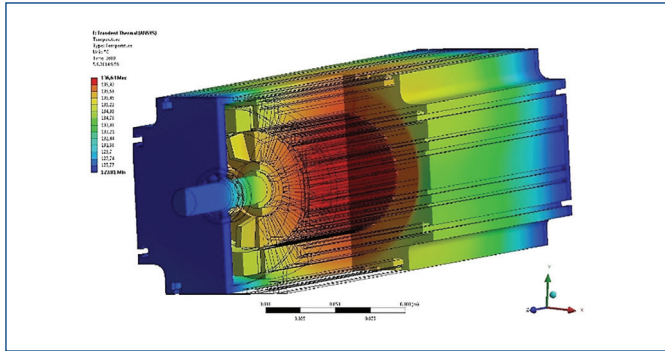


Figure 4. Temperatures distribution

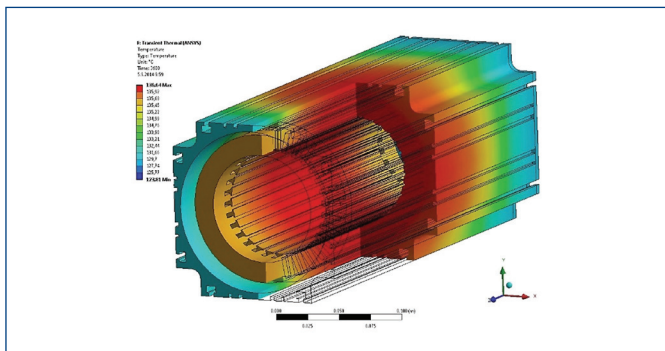


Figure 5. Temperatures distribution at stator

straight winding parts and the overhang winding parts. Minimum steady-state value of temperature stator overhang winding is 130 °C. Stator winding has maximum steady-state temperature 134 °C. Highest final temperature of winding is at straight parts. Result shows small temperature difference between straight stator winding part and stator iron core.

Fig. 6. presents the final temperature distribution at the rotor parts. Minimum final temperature of rotor windings is 124 °C. Maximum final temperature of rotor bars is 136 °C. At this place have to be mentioned steady-state temperatures of bearings. Steady-state temperature of non-drive end (NDE) bearing is 130 °C. Steady-state temperature of drive end (DE) bearing is 126 °C.

5. CONCLUSION

This paper presents a 3D coupled transient thermal analysis. The theoretical background and physical laws are presented in an abstract. Thermal analysis is based on coupled CFD and FEM model. Theoretical bases are applied at new designed IM. The nominal power 9 kW and mains dimensions of IM are based on existing PMSM.

3D coupled thermal analysis used CFD to determinate boundary condition. 3D coupled model describes IM's unsymmetrical and

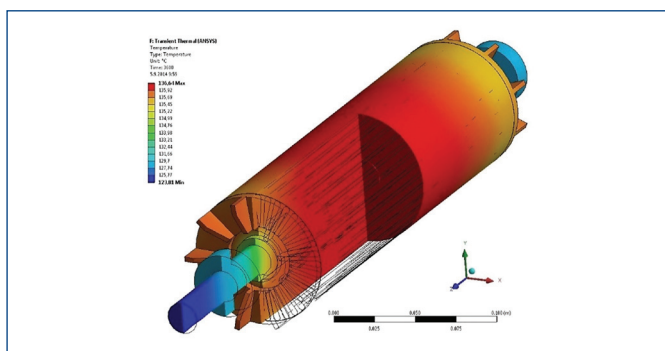


Figure 6. Temperatures distribution of rotor IM

simulations are complex. The heat transfer coefficient is calculated and then implemented to thermal model as boundary condition at cooling surface. Advantage of presented method is in elimination of air ambient in transient thermal analysis. This fact leads to saving of computing times.

Losses of IM are calculated on the basis of knowledge of the magnetic circuit geometry and distribution of electromagnetic fields.

The final temperature range of motor is from 123 °C to 136 °C. The maximum steady-state temperature of stator winding is 134 °C. According to thermal analysis results, IM can operate in insulation class H without thermal damage. The presented paper has practical significance for designers of electrical machines.

ACKNOWLEDGEMENTS

This research has been supported by the European Regional Development Fund and the Ministry of Education, Youth and Sports of the Czech Republic under the Regional Innovation Centre for Electrical Engineering (RICE), project no. CZ.1.05/2.1.00/03.0094, TAČR project no. TA0200103 CIDAM and funding program SGS-2012-071.

REFERENCES

- [Alberti 2008] Alberti, L., Bianchi, N. A Coupled Thermal-Electromagnetic Analysis for a Rapid and Accurate Prediction of IM Performance, IEEE Transactions on Ind Electron, vol. 55, pp. 3575-3582, Oct 2008.
- [Hruska 2012] Hruska, K., Kindl, V., Pechanek, R. Design and FEM analyses of an electrically excited automotive synchronous motor, Power Electronics and Motion Control Conference (EPE/PEMC), 2012 15th International, vol., no., pp.LS2e.2-1, LS2e.2-7, 4-6 Sept. 2012
- [Kindl 2010] Kindl, V., Pechanek, R., Bouzek, L. Cooling of new designed machine, MECHATRONIKA, 2010 13th International Symposium, vol., no., pp. 95, 98, 2-4 June 2010
- [Kolondzovski 2010] Kolondzovski, Z., Sallinen, P., Arkkio, A. Thermal analysis of a high-speed PM machine using numerical and thermal-network method, ICEM 2010 – XIX International Conference on Electrical Machines, vol., no., pp.1, 6, 6-8 Sept. 2010
- [Kuosa 2004] Kuosa, M., Sallinen, P. and Larjola, J. Numerical and experimental modeling of gas flow and heat transfer in the air gap of an electric machine, Journal of Thermal Science, vol. 13, pp. 264-278, Aug. 2004.
- [Marignetti 2008] Marignetti, F. et al. Design of Axial Flux PM Synchronous Machines Through 3-D Coupled Electromagnetic Thermal and Fluid-Dynamical Finite-Element Analysis, IEEE Transactions on Industrial Electronics, vol. 55, pp. 3591-3601, Oct 2008.
- [Staton 2005] Staton, D., Boglietti, A., Cavagnino, A. Solving the More Difficult Aspects of Electric Motor Thermal Analysis in Small and Medium Size Industrial Induction Motors, Energy Conversion, IEEE Transactions on, vol.20, no. 3, pp.620, 628, Sept. 2005
- [Trigeol 2006] Trigeol, J. F., Bertin, Y. and Lagonotte, P. Thermal modeling of an induction machine through the association of two numerical approaches, IEEE Trans. Energy Conversion, vol. 21, pp. 314-323, Jun. 2006.
- [Vlach 2010] Vlach, R. Heating Prediction of Electric Machine Using Neural Network, MENDEL 2010 – 16th International Conference on Soft Computing. Brno. 2010. p. 298 – 302. ISBN 978-80-214-4120-0.
- [Zhang 2012] Zhang, Y., Sun, M., Ruan, J., Huang, T. Ventilation Structure Improvement of Large Motors Using 3-D Multi-Physical Coupled-Field Finite-Element Analysis, ICEF 2012 – 6th International Conference on Electromagnetic Field Problems and Applications, vol., no., pp. 1,4, 19-21 June 2012.

CONTACT

Ing. Roman Pechanek, Ph.D.
 Faculty of Electrical Engineering
 Regional Innovation Centre for Electrical Engineering
 University of West Bohemia,
 Univerzitní 26, 306 14 Plzeň, Czech Republic
 e-mail: rpechane@rice.zcu.cz, www.rice.cz